

Measuring acoustic nonlinearity parameter using collinear wave mixing

Minghe Liu,¹ Guangxin Tang,² Laurence J. Jacobs,³ and Jianmin Qu^{1,2,a)}

¹Department of Civil and Environmental Engineering, Northwestern University, Evanston, Illinois 60208, USA

²Department of Mechanical Engineering, Northwestern University, Evanston, Illinois 60208, USA

³College of Engineering, Georgia Institute of Technology, Atlanta, Georgia 30332-0360, USA

(Received 9 May 2012; accepted 27 June 2012; published online 30 July 2012)

This study introduces a new acoustic nonlinearity parameter β_T . It is shown that β_T is associated with the interaction between a longitudinal wave and a shear wave in isotropic elastic solids with quadratic nonlinearity. Experimental measurements are conducted to demonstrate that the collinear wave mixing technique is capable of measuring β_T nondestructively. Further, it is shown that β_T is well-correlated with the plastic deformation in Al-6061 alloys. These results indicate that collinear wave mixing is a promising method for nondestructive assessment of plastic deformation, and possibly, fatigue damage in metallic materials. © 2012 American Institute of Physics.

[<http://dx.doi.org/10.1063/1.4739746>]

I. INTRODUCTION

Extensive experimental data have demonstrated that the acoustic nonlinearity parameter β is closely related to the degree of fatigue damage in metallic materials, thus by measuring β , it is possible to assess fatigue damage.^{1–7} Because of this discovery, various techniques have been developed and refined in recent years to measure β . One of the techniques most often used is the generation of second harmonics. In this method, either a longitudinal wave, a Rayleigh surface wave, or a Lamb wave of a certain frequency is launched into a sample by a transducer, and the interaction between this incident wave and material nonlinearities in the sample generates a corresponding second harmonic wave. Since the amplitude of the second harmonic wave is proportional to β , by measuring the amplitude of the second harmonic, β can be experimentally obtained.

There are, however, some drawbacks inherent to the method of generation of second harmonics. First, the technique measures the average β over the region between the transducer and the receiver. Therefore, spatial resolution is limited. Second, there are many extraneous sources of second harmonics besides material nonlinearity, and these can be easily generated by the instrumentation of the measurement system, such as the transducers, couplants, amplifiers, etc. Therefore, the second harmonic signal recorded by the receiver may not all be due to the material nonlinearity of the sample. Some of this measured nonlinearity may be due to the nonlinearity of the measurement system, which reduces the accuracy of the method.

To overcome these limitations of the method of generation of second harmonics, Croxford *et al.* had recently reported the application of a non-collinear mixing technique to the ultrasonic measurement of material nonlinearity to assess plasticity and fatigue damage.⁸ This method is based on the fact that a resonant wave might be generated by two incident waves if certain conditions are satisfied. Among other parameters, the amplitude of the generated resonant

wave is related to the material nonlinearity. Therefore, by measuring the generated resonant wave, material nonlinearity might be obtained. This idea was first discussed by Jones *et al.*⁹ and experimentally verified later by Rollins,¹⁰ and Johnson *et al.*¹¹ As pointed out by Croxford *et al.*,⁸ the wave mixing method is less sensitive to measurement system nonlinearities, and allows for great flexibility in selecting the wave modes, frequencies, and propagating directions.

However, it is crucial to note that, depending on the types of wave mixing method used, the measured material nonlinearity may not be exactly the same as the acoustic nonlinearity parameter β commonly used in the nonlinear acoustic literature. This can be understood from the fact that the nonlinearity of an isotropic elastic solid is described by three independent third order elastic (TOE) constants. Therefore, it is possible that there needs to be three independent acoustic nonlinearity parameters to fully describe the (quadratic) nonlinear behavior of an isotropic elastic solid. The β commonly referred to in the literature is possibly only one of these three nonlinearity parameters. A recent study by Tang *et al.*¹² has identified, in addition to β which is associated with longitudinal waves, another independent acoustic nonlinearity parameter β_S which is associated with the second harmonic shear wave induced by the mode conversion from the fundamental longitudinal to shear at an interface. As will be shown in this paper, yet another independent acoustic nonlinearity parameter β_T needs to be introduced in order to describe the interaction between a longitudinal wave and a shear wave. We note that, in addition to the three independent Murnaghan coefficients, there are also two independent Lamé constants. The three acoustic nonlinearity parameters, β_T , β_L , and β_S are independent combinations of these five elastic constants. It is in this sense that β_T , β_L , and β_S are independent.

The questions that naturally arise are (1) can these additional acoustic nonlinearity parameters be measured? and (2) are these additional acoustic nonlinearity parameters related to material damage such as plastic deformation and fatigue in metallic materials? In this study, we demonstrate that the acoustic nonlinearity parameter β_T can be measured by using

^{a)}Electronic mail: j-qu@northwestern.edu.

a collinear wave mixing method, and β_T is indeed related to plastic deformation in an aluminum alloy. The paper is arranged as follows. In Sec. II, asymptotic solutions are derived for the interaction between a longitudinal and a shear wave propagating in opposite directions, from which β_T is introduced. In Sec. III, numerical simulations are conducted to verify that the conclusions from Sec. II which are based on steady-state time harmonic waves are also valid for transient pulses of finite durations. Experimental setup and the method of wave mixing to measure β_T are described in Sec. IV. Finally, in Sec. V, we demonstrate experimentally that β_T is indeed related to plastic deformation in the Al6061, indicating feasibility of using β_T to assess damage in metallic materials.

II. ASYMPTOTIC SOLUTION OF NONLINEAR WAVE MIXING

Consider two plane waves propagating collinearly in opposite directions in an elastic media with quadratic nonlinearity. Without loss of generality, we assume that the waves are propagating along the y -direction in a Cartesian coordinate system (x, y) , and the particle motion can be either in the x - or the y -direction. Let $u(y, t)$ and $v(y, t)$ be the displacement components in the x - and the y -directions, respectively. Then, the governing equations of motion can be written as

$$\frac{\partial \sigma_{xy}}{\partial y} = \rho \frac{\partial^2 u}{\partial t^2}, \quad \frac{\partial \sigma_{yy}}{\partial y} = \rho \frac{\partial^2 v}{\partial t^2}, \quad (1)$$

where ρ denotes the mass density, and σ_{xy} and σ_{yy} denote the stress components. In terms of the Lamé constants λ and μ , and the third order elastic constants l , m , and n (the Murnaghan coefficients), the stress components can be related to the displacement gradients through,¹³

$$\sigma_{yy} = (\lambda + 2\mu) \frac{\partial v}{\partial y} + (l + 2m) \left(\frac{\partial v}{\partial y} \right)^2 + \frac{m}{2} \left(\frac{\partial u}{\partial y} \right)^2, \quad (2)$$

$$\sigma_{xy} = \sigma_{yx} = \frac{\partial u}{\partial y} \left(\mu + m \frac{\partial v}{\partial y} \right). \quad (3)$$

Substituting Eqs. (2) and (3) into Eq. (1) leads to the following nonlinear partial differential equations,

$$\frac{\partial^2 u}{\partial t^2} - c_T^2 \frac{\partial^2 u}{\partial y^2} = \beta_T c_T^2 \frac{\partial}{\partial y} \left(\frac{\partial u}{\partial y} \frac{\partial v}{\partial y} \right), \quad (4)$$

$$\frac{\partial^2 v}{\partial t^2} - c_L^2 \frac{\partial^2 v}{\partial y^2} = \beta_L c_L^2 \frac{\partial v}{\partial y} \frac{\partial^2 v}{\partial y^2} + \beta_T c_T^2 \frac{\partial u}{\partial y} \frac{\partial^2 u}{\partial y^2}, \quad (5)$$

where $c_L = \sqrt{(\lambda + 2\mu)/\rho}$ and $c_T = \sqrt{\mu/\rho}$ are the longitudinal and shear wave velocities, respectively, and

$$\beta_L = 3 + \frac{2(l + 2m)}{\lambda + 2\mu}, \quad \beta_T = \frac{\lambda + 2\mu}{\mu} + \frac{m}{\mu} \quad (6)$$

can be viewed as the acoustic nonlinear parameters. We note that β_L in Eq. (6) is the β commonly used in the literature for longitudinal waves.

Now, consider a time-harmonic shear wave of frequency ω_T and amplitude U propagating in the positive y -direction and a time-harmonic longitudinal wave of frequency ω_L and amplitude V propagating in the negative y -direction, see Fig. 1. If the two frequencies satisfy the following equation:

$$\frac{\omega_L}{\omega_T} = \frac{2c_L}{c_L - c_T}, \quad (7)$$

then, an asymptotic solution to Eqs. (4) and (5) can be written as

$$u(y, t) = U \sin \left[\omega_T \left(t - \frac{y}{c_T} \right) \right] + u_2(y, t), \quad (8)$$

where we have neglected the higher order terms that do not grow with propagation distance, and

$$u_2(y, t) = A \cos \left[\omega_R \left(t + \frac{y}{c_T} \right) \right], \quad A = \frac{\beta_T UV \omega_T^2}{2c_T(c_L - c_T)} y, \quad (9)$$

$$\omega_R = \frac{c_L + c_T}{c_L - c_T} \omega_T.$$

The $u_2(y, t)$ above is called a resonant wave induced by nonlinear wave mixing. This resonant wave is a shear wave propagating in the negative y -direction with phase velocity c_T . If $u_2(y, t)$ can be measured experimentally, i.e., A is known, then the nonlinear acoustic parameter β_T can be evaluated by the following equation:

$$\beta_T = \frac{2c_T(c_L - c_T)}{UV \omega_T^2 y} A. \quad (10)$$

III. NUMERICAL SIMULATIONS OF NONLINEAR WAVE MIXING

The asymptotic solution derived in the previous section is for infinite wave trains. In practice, the two primary waves are likely to be wave packets with finite length. To verify that the resonant wave still exists even when two wave packets of finite length are mixed, we develop in this section a numerical procedure based on the finite difference method to simulate the collinear mixing of a longitudinal packet and a shear wave packet in a solid with quadratic nonlinearity.

To carry out the numerical analysis, it is convenient to reformulate Eqs. (4) and (5) into a hyperbolic system of

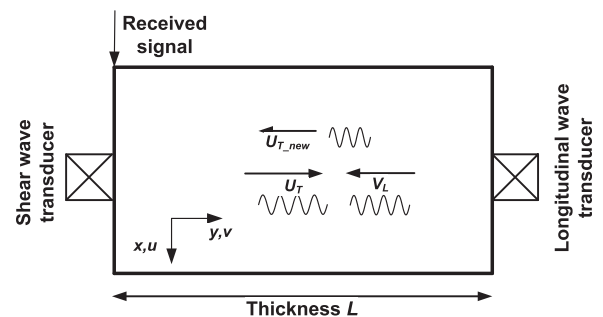


FIG. 1. Two wave mixing in a nonlinear material.

conservation laws defined in a one-dimensional domain $y \in (0, L)$, where L is the sample length,

$$\frac{\partial}{\partial t} \hat{q} + \frac{\partial}{\partial y} \hat{f}(\hat{q}) = 0, \quad (11)$$

where

$$\hat{q}(x, y, t) = \begin{bmatrix} q^{(1)}(x, y, t) \\ q^{(2)}(x, y, t) \\ q^{(3)}(x, y, t) \\ q^{(4)}(x, y, t) \end{bmatrix} = \begin{bmatrix} \partial u / \partial t \\ \partial v / \partial t \\ \partial u / \partial y \\ \partial v / \partial y \end{bmatrix},$$

$$\hat{f}(x, y, t) = \begin{bmatrix} -\frac{1}{\rho} \sigma_{xy}(q^{(3)}, q^{(4)}) \\ -\frac{1}{\rho} \sigma_{yy}(q^{(3)}, q^{(4)}) \\ -q^{(1)} \\ -q^{(2)} \end{bmatrix}. \quad (12)$$

Equation (11) can be solved using an explicit second-order Runge-Kutta method, or the modified Euler method.¹⁴ In this work, the numerical solution algorithm is implemented using the library CENTPACK.¹⁵

The boundary conditions are implemented using the ghost-cell method,¹³ which is integrated in CENTPACK. The shear wave source is to simulate the shear wave transducer which generates and receives shear waves. The material parameters used in the numerical simulations are listed in Table I, and L is taken as 72.2 mm. Those parameters are a fairly good approximation of aluminum alloys.¹⁶ By delaying the start of the longitudinal wave by 8 μ s, the primary shear and longitudinal waves meet in the middle of the sample. The wave packets are short enough so that they will not interfere with the resonant wave generated by the mixing.

Based on the parameters listed in Table I, the resonant condition Eq. (7) yields $\omega_L = 3.987 \omega_T$ and $\omega_R = 2.987 \omega_T$. If ω_T is 2.5 MHz, then $\omega_L = 9.97$ MHz and $\omega_R = 7.47$ MHz. The corresponding simulated time-domain signal recorded by the shear transducer is shown in Fig. 2(a). The first portion up to about 12 μ s is the 30 cycle sinusoidal input signal to generate the shear wave. The second portion, starting at around 22 μ s is the resonant shear wave generated by the mixing of the primary shear and longitudinal waves. Fig. 2(b) shows an enlarged view of this resonant wave. The diamond shape of the signal is expected because as the two primary wave packets approach each other, their mixing zone starts from zero when the two packets first come in contact, then reaches a maximum when the two wave packets are fully overlapped, and decreases to zero when the two wave packets pass each other. This also confirms that the amplitude of the resonant wave is linearly proportional to the size of the mixing zone. Carrying out the fast Fourier transform in conjunction with a

Hanning window over the resonant wave gives the frequency spectrum, see Fig. 2(c). Clearly, the central frequency is 7.47 MHz as expected of the resonant wave.

The numerical solutions confirm that even when the two primary waves are wave packets of finite duration, their mixing still generates a resonant shear wave that propagates back to the shear wave transducer, as long as the resonant condition (7) is satisfied. The amplitude of the resonant shear wave is proportional to the zone size over which the two primary wave packets mix.

IV. EXPERIMENTAL MEASUREMENT

Experimental measurements are conducted on samples made of Al-6061. The samples are cubes with 76.2 mm on each side. To align the transducers, two dents of 2 mm deep are made on two opposite sides of the specimen surface. Thus, the effective thickness of these samples is 72.2 mm, the same as in our numerical calculation. A schematic of the nonlinear collinear beam-mixing measurement setup is shown in Fig. 3. The high power gated amplifier RAM-5000 SNAP (RITEC Inc, Warwick, RI) with two “RF burst” channels is used to drive both longitudinal and shear wave transducers. The internal trigger signal from the RAM-5000 SNAP is used as a reference trigger. As shown in Fig. 3, the two source waves propagate through the material and intersect with each other in a comparatively long zone, and the generated third shear wave is received by the shear wave transducer. This function is enabled by the RDX-6 diplexer (RITEC Inc., Warwick, RI). The resonant shear wave is digitized by a Tektronix TDS 5034B oscilloscope with a sampling frequency of 625 MHz and 25 000 sample points with 250 times average to increase the signal-to-noise ratio (SNR). The digitized time-domain signal is then sent to a PC for post signal processing.

A broad-band Piezoelectric Transducer (PZT) shear wave transducer with a center frequency of 5 MHz is used as both the transmitter and the receiver. Another broad-band PZT longitudinal transducer with a center frequency of 10 MHz is used to generate the longitudinal wave. Excitation signals into both input transducers are 30-cycles tone bursts at 500 V. Measurements are performed on fixed shear wave frequency ω_T and variable longitudinal wave frequency ω_L to generate both the resonance and non-resonance conditions, and to obtain the bandwidth of the generated resonance.

To isolate the wave generated by the mixing, time-domain signals of the two primary waves are subtracted from the total time-domain signal received by the shear wave transducer. The resulting signal is then transformed into the frequency domain by the fast Fourier transform. According to our numerical calculations in Sec. III, the generated shear wave should arrive at the shear wave transducer at about 22 μ s and its duration is about 8 μ s. Therefore, we

TABLE I. Material and input parameters.

ρ (kg/m ³)	λ (N/m ²)	μ (N/m ²)	l (N/m ²)	m (N/m ²)	f_T (MHz)	N_c	Q (m)
2719	5.43×10^{10}	2.68×10^{10}	-38.75×10^{10}	-35.8×10^{10}	2.5	30	1×10^{-8}

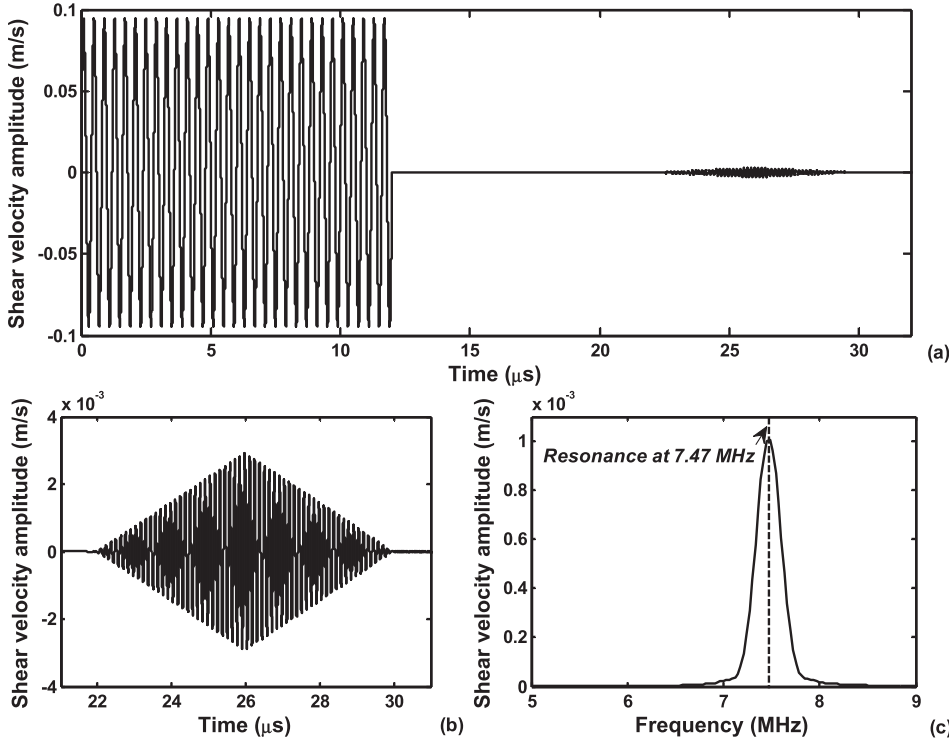


FIG. 2. (a) Time-domain signals registered on the shear wave transducer, (b) time-domain signals of the resonant wave, and (c) frequency spectrum of the resonant wave.

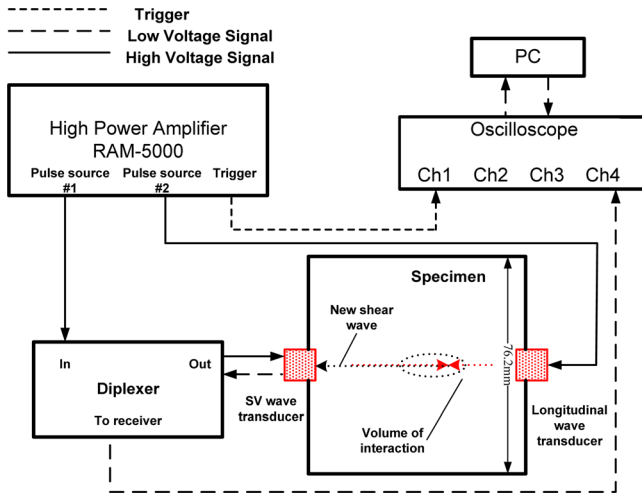


FIG. 3. Experimental setup.

carry out the Fourier transform of the total time-domain signal received by the shear wave transducer during this period of time, after removing the time-domain signals of the primary shear and longitudinal waves. The corresponding frequency spectrum is shown in Fig. 4 for $\omega_T = 2.5$ MHz with $\omega_L = 9.97$ MHz, 8.5 MHz, and 11 MHz, respectively. Among these three cases, only $\omega_L = 9.97$ MHz meets the resonance condition. It is clear in Fig. 4 that only when $\omega_L = 9.97$ MHz is the generated shear wave a resonant wave that shows a significant peak at 7.87 MHz. For the other two cases, there is no resonant wave, and all the frequency components near 7.87 MHz are within the noise level.

V. APPLICATIONS OF THE COLLINEAR WAVE MIXING TECHNIQUE

In our measurements, the shear wave frequency is fixed and longitudinal wave frequency varies around the resonance

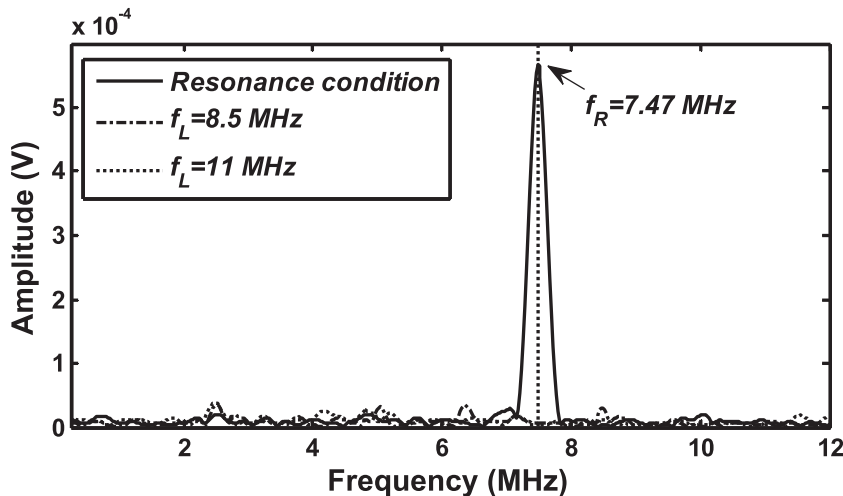


FIG. 4. Frequency spectrum of the generated shear wave for $\omega_L = 9.97$ MHz, 8.5 MHz, and 11 MHz, respectively. All for $\omega_T = 2.5$ MHz.

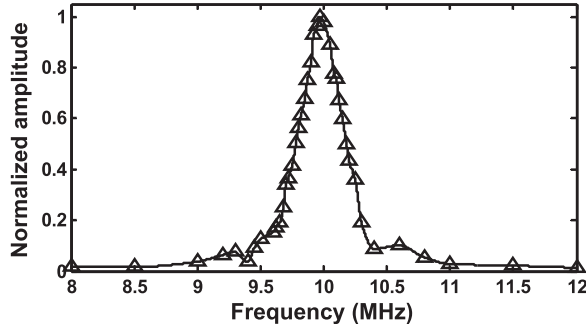


FIG. 5. Bandwidth of resonance wave for Al-6061 specimen.

frequency from 8 MHz to 12 MHz. The amplitude of the shear wave generated by wave mixing is normalized by its maximum value and plotted in Fig. 5 as a function of longitudinal wave frequency. When the longitudinal wave frequency is 9.97 MHz, the generated shear wave is at resonance, as clearly shown in Fig. 5. We note that the resonance wave has a rather narrow bandwidth, ~ 0.4 MHz, which corresponds to a Q-factor of ~ 25 . This is a very nice feature and may have potential application for measuring material properties accurately, or for building mechanical oscillator with a high Q-factor.

It follows from Eq. (10) that the acoustic nonlinearity parameter β_T can be estimated if the amplitude of the resonant shear wave is measured experimentally. Extensive analytical and experimental studies have demonstrated that the acoustic nonlinearity parameter β_L is well correlated with the amount of plastic deformation in metallic materials.^{3,4,17–20} One objective of the current study is to determine if β_T can also be related to plastic deformation.

To this end, four Al-6061 samples were subjected to different degree of compressive plastic deformation. Ultrasonic measurements are then performed on those samples using the collinear wave mixing technique described in Sec. IV. The amplitude of the resonant shear wave is measured in the direction transverse to the loading direction. The corresponding acoustic nonlinearity parameter β_T is then estimated from the amplitude of the resonant shear wave by using Eq. (10). The measured β_T is normalized by the corresponding value of the undeformed sample, and is plotted in Fig. 6 as a function of the plastic strain in the sample. The error

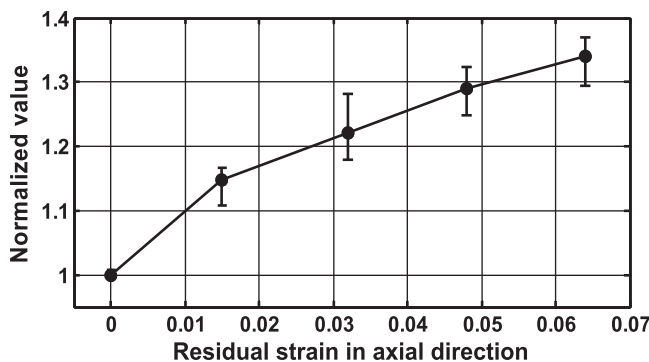


FIG. 6. Normalized nonlinear parameter ($\beta_T/\beta_{undamaged}$) for Al-6061 samples with different amount of plastic deformation.

bars are obtained through six measurement points on each specimen. It can be clearly seen that β_T increases significantly with increasing plastic strain. At 1.5% plastic strain, there is more than a 14% increase in β_T . At 6.5% plastic strain, the increase in β_T is almost 35%. Clearly, the collinear wave mixing method developed in this study provides a sensitive tool to measure β_T , and consequently estimate plastic deformation in metallic materials.

VI. CONCLUSION

This study investigates the feasibility of using a collinear wave mixing technique to measure the acoustic nonlinearity parameter, β_T . We found that the wave mixing method has the potential to measure the acoustic nonlinearity parameter without many of the experimental difficulties inherent to some of the existing second harmonic methods. Chief among them is the ability to select the resonant frequency that does not coincide with those associated with typical measurement systems. Therefore, the collinear mixing technique has higher sensitivity in measuring the acoustic nonlinearity parameter. Further, we demonstrated that β_T is well-correlated with the amount of plastic deformation in the material. It is possible to nondestructively estimate plastic deformation in metallic materials by measuring β_T . Finally, although not reported in this paper, the wave mixing technique allows the measurement over a specific region of interest in the specimen. This capability makes it possible to obtain the spatial distribution of β_T through the thickness direction of the sample by timing the transducers.

Before closing, it should also be pointed out that although the collinear mixing technique used in this study requires only two transducers as opposed to three transducers typically needed for non-collinear mixing techniques, it does have some limitations. For example, it requires that the shear wave transducer to have a rather broad bandwidth, because the frequency of the resonant shear wave in a typical solid is about 3 times of that of the fundamental shear wave. This also limits the flexibility in selecting the resonant frequencies in order to avoid system nonlinearities.

ACKNOWLEDGMENTS

The research was supported in part by the National Science Foundation under CMMI-0653883.

¹P. B. Nagy, *Ultrasonics* **36**(1-5), 375–381 (1998).

²J. H. Cantrell and W. T. Yost, *Int. J. Fatigue* **23**, S487–S490 (2001).

³C. Bernes, J. Y. Kim, J. Qu, and L. J. Jacobs, *Appl. Phys. Lett.* **90**(2), 021901 (2007).

⁴C. Pruell, J. Y. Kim, J. Qu, and L. J. Jacobs, *Appl. Phys. Lett.* **91**, 231911 (2007).

⁵M. F. Muller, J. Y. Kim, J. Qu, and L. J. Jacobs, *J. Acoust. Soc. Am.* **127**(4), 2141–2152 (2010).

⁶K. H. Matlack, J. Y. Kim, L. J. Jacobs, and J. Qu, *J. Appl. Phys.* **109**(1), 014905 (2011).

⁷Y. Liu, J. Y. Kim, L. J. Jacobs, J. Qu, and Z. Li, *J. Appl. Phys.* **111**(5), 053511 (2012).

⁸A. J. Croxford, P. D. Wilcox, B. W. Drinkwater, and P. B. Nagy, *J. Acoust. Soc. Am.* **126**(5), E1117–E1122 (2009).

⁹G. L. Jones and D. R. Korbett, *J. Acoust. Soc. Am.* **35**(1), 5–10 (1963).

¹⁰F. R. Rollins, *Appl. Phys. Lett.* **2**(8), 147–148 (1963).

- ¹¹P. A. Johnson and T. J. Shankland, *J. Geophys. Res. [Solid Earth Planets]* **94**(B12), 17729–17733, doi:10.1029/JB094iB12p17729 (1989).
- ¹²G. Tang, L. J. Jacobs, and J. Qu, *J. Acoust. Soc. Am.* **131**(4), 2570–2578 (2012).
- ¹³S. Kuchler, T. Meurer, L. J. Jacobs, and J. Qu, *J. Acoust. Soc. Am.* **125**(3), 1293–1301 (2009).
- ¹⁴C. F. Gerald and P. O. Wheatley, *Applied Numerical Analysis* (Addison-Wesley, MA, 1989), pp. 356–360.
- ¹⁵J. Balbas and E. Tadmor, CENTPACK, available at <http://www.cscamm.umd.edu/centpack/software>, last viewed April 2010.
- ¹⁶R. T. Smith, R. Stern, and R. W. Stephens, *J. Acoust. Soc. Am.* **40**(5), 1002–1008 (1966).
- ¹⁷J. Herrmann, J. Y. Kim, L. J. Jacobs, J. Qu, J. W. Little, and M. F. Savage, *J. Appl. Phys.* **99**(12), 124913 (2006).
- ¹⁸G. Shui, J. Y. Kim, J. Qu, Y. S. Wang, and L. J. Jacobs, *NDT & E Int.* **41**(5), 326–329 (2008).
- ¹⁹C. Pruell, J. Y. Kim, J. Qu, and L. J. Jacobs, *NDT & E Int.* **42**(3), 199–203 (2009).
- ²⁰M. Liu, J. Y. Kim, L. Jacobs, and J. Qu, *NDT & E Int.* **44**(1), 67–74 (2011).